The Journal of Physical Chemistry A

 VOLUME 101, NUMBER 9, FEBRUARY 27, 1997

ARTICLES

Investigation of the Photoinduced Electron Transfer Reaction between 9,10-Dicyanoanthracene and 1-Methylnaphthalene in Acetonitrile Using Picosecond Transient Grating Spectroscopy

Eric Vauthey*,†

Institute of Physical Chemistry of the University of Fribourg, Pérolles, CH-1700 Fribourg, Switzerland

Received: June 20, 1996; In Final Form: November 5, 1996[⊗]

A spectroscopic and kinetic study of the photoinduced electron transfer (ET) reaction between 9,10-dicyanoanthracene (DCA) and 1-methylnaphthalene (MNA) in acetonitrile using the transient grating technique is reported. Apart from the bands assigned to ^{1}DCA* and DCA$^{\bullet-}$, the transient spectrum exhibits a band located at 580 nm and ascribed to $MNA_2^{\bullet+}$. This species is generated upon reaction of a second donor molecule with a 1:1 complex to form a 1:2 complex ($DCA^{\bullet-}\cdot MNA_2^{\bullet+}$). Using chloranil as electron acceptor, the rate constant of this reaction has been measured to be 6.8×10^9 M^{-1} s^{-1}. From the donor concentration dependence of the kinetics of DCA$^{\bullet-}$ diffraction intensity and of the free ion yield, the rates of back ET to the ground state within the 1:1 and the 1:2 complexes have been determined to be equal to 1.8×10^8 and 16.9×10^8 s^{-1}, respectively, while their rate constants of separation into free ions are 1.6×10^8 and 1.1×10^8 s^{-1}, respectively. These values have been obtained assuming a reaction scheme in which both forward and backward ET essentially take place at contact distance. In the case of the 1:1 complex, however, charge recombination within a loose ion pair cannot be ruled out.

Introduction

Over the past decades, intermolecular photoinduced electron transfer (ET) reactions have been very intensively studied.[1] Two ET processes are involved in the simplest reaction scheme. The first one is the forward ET which results in the fluorescence quenching of the excited reaction partner. The second is the back ET to the neutral ground state taking place within the geminate ion pair formed upon quenching. In the end of the 1980s, this process was used to test Marcus theory. In many cases, the rate constant of back ET, k_{bet}, was not measured directly but was calculated from the experimentally determined free ion yield and by assuming a constant value for the rate constant of separation of the geminate ion pair into free ions, k_{sep}, of 5×10^8 s^{-1}.[2,3] Recently, it has been shown that, in some cases, the species produced upon ET quenching in MeCN exhibits exciplex fluorescence.[4] In a recent paper, Gould and Farid showed that the exciplex fluorescence intensity as well as the free ion yield decreases substantially with increasing donor concentration, when the donor is naphthalene or a methyl-substituted naphthalene.[5] This effect was ascribed to the reaction of the exciplex with a second donor molecule to form a 1:2 complex with the donor dimer radical cation ($A^{\bullet-}\cdot D_2^{\bullet+}$), where back ET is faster. The rate constants of back ET within these species were estimated from the combination of free ion yields and steady state fluorescence measurements, and by assuming a reaction scheme involving both 1:1 and 1:2 contact ion pairs (CIP) and solvent separated or loose ion pairs (LIP).

In nonpolar solvents, a decrease of the exciplex fluorescence lifetime and quantum yields with increasing quencher concen-

† E-mail: Eric.Vauthey@unifr.ch.

⊗ Abstract published in *Advance ACS Abstracts*, February 1, 1997.

S1089-5639(96)01853-1 CCC: $14.00

tration has also been observed with various donors such as triethylamine[6] and dimethylaniline.[7] This effect has been ascribed to the formation of a triplex, which is, in most cases, nonfluorescent. One of the only triplex luminescence reported in the literature was observed with tetracyanoethylene and naphthalene in toluene.[8]

In this paper, we present direct measurements of the rate constant of deactivation of the complexes formed upon ET quenching of the excited electron acceptor 9,10-dicyanoanthracene (DCA) by 1-methylnaphthalene (MNA) in acetonitrile (MeCN), using transient grating (TG) spectroscopy. MNA was preferred to naphthalene for its high solubility in MeCN. The details of TG spectroscopy are described in ref 9. One advantage of this method over transient absorption spectroscopy is its superior sensitivity,[9] which allows the detection of transient species with low extinction coefficients, such as $MNA^{\bullet+}$, without using too high excitation intensities, at which undesired nonlinear optical processes can occur. These data will be combined with the free ion yields to deduce the rate constants of back ET within the 1:1 and 1:2 complexes as well as their rate constants of separation into free ions.

Experimental Section

Apparatus. The picosecond TG setup has been described in detail previously.[10,11] Briefly, the third harmonic output at 355 nm of an active/passive mode-locked Q-switched Nd:YAG laser (Continuum Model PY61-10) was split in two parts, which, after traveling through different paths of equal lengths, were crossed on the sample with an angle of 0.3°. Two different probing schemes were used:

1. In the spectroscopic mode, a 15 mJ pulse at 1064 nm was sent along a variable optical delay line before being focused into a 25 cm long cell filled with a 60:40 (v/v) D_2O/H_2O mixture. The resulting white light pulses were collimated on the sample with an angle of incidence of 0.25°. The diffracted signal was focused in a light guide connected to the entrance of a $^1/_4$ m imaging spectrograph (Oriel Multispec). As detector, a 1024 × 256 pixels water-cooled CCD camera (Oriel Intaspec IV) was used.

2. In the kinetic mode, a pulse at 532 nm was sent along the variable optical delay line before being Raman shifted to 681 nm in deuterated DMSO. The diffracted pulse was filtered through a 650 nm cutoff filter and reflected into a vacuum photodiode. At each position of the delay line, the diffracted intensity was averaged over 20 laser pulses. For each measurements, the delay line was scanned eight times. Each measurement was repeated three times and the average value was used. The duration of the pulses was about 30 ps. The total pump intensity on the sample was around 2 mJ/cm^2 and the probe pulse intensity was at least 10 times smaller. The polarization of the probe pulse was oriented at 54.7° relative to the polarization of the pump pulses.

The free ion yields were determined using photoconductivity.[12] The photocurrent cell has been described in detail elsewhere.[13] The system benzophenone with 0.02 M 1,2-diazabicyclo[2.2.2]octane in MeCN, which has a free ion yield of unity,[14] was used as a standard.

Samples. 1,2-Diazabicyclo[2.2.2]octane (DABCO, Fluka) and 9,10-dicyanoanthracene (DCA, Aldrich) were purified by sublimation. Chloranil (CA, Fluka) was twice recrystallized from benzene. 1-Methylnaphthalene (MNA, Fluka) was refluxed on BaO and vacuum distilled.[15] Benzophenone (BP, Aldrich Gold Label) and acetonitrile (MeCN, Fluka UV grade) were used without further purification. During sample preparation, great care was taken to avoid water contamination.[16] For TG experiments, the absorbance of the sample solution at 355 nm was around 0.15 on 1 mm, the cell thickness. For photoconductivity, the sample absorbance was around unity on 1 cm. All measurements were performed at 20 ± 1 °C.

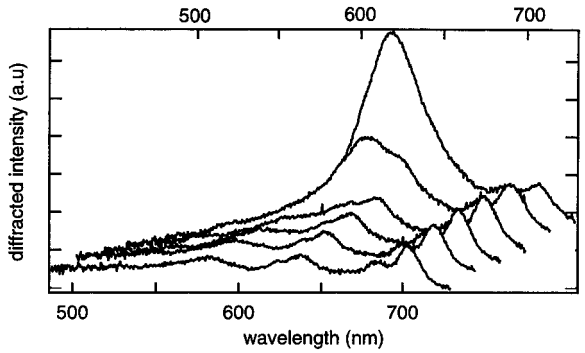

Figure 1. Diffracted spectra measured at different time delays after excitation at 355 nm of a solution of DCA and 0.2 M MNA in MeCN (from top to bottom: Δt = 100, 400, 800, 950, 1100, and 1500 ps). The bottom and top wavelength axes refer to the bottom and top TG spectra, respectively.

Results

Figure 1 shows the transient grating spectra obtained at different time delays after excitation at 355 nm of a solution of DCA with 0.2 M MNA in MeCN. The band at 620 nm, which corresponds to ^{1}DCA* absorption, decays rapidly as a consequence of ET quenching, which is diffusion controlled according to fluorescence measurements ($k_q = 1.7 \times 10^{10}$ M^{-1} s^{-1}). At high donor concentrations, a broadening of the red edge of DCA $S_1 \leftarrow S_0$ absorption band (around 440 nm), indicating the formation of a ground state complex, is observed. However, as the excitation wavelength is located on the blue side of this absorption band, ET occurs almost completely upon bimolecular quenching. Coming back to Figure 1, the spectrum of ^{1}DCA* is rapidly replaced by another spectrum which contains a band with a shoulder located around 700 nm and two other bands at 640 and 580 nm. Apart from the latter band, this spectrum is identical with that obtained using a donor, whose cation absorbs below 500 nm.[9] Consequently, these bands can be safely assigned to $DCA^{\bullet-}$.[17] From this spectrum it is not possible to specify whether $DCA^{\bullet-}$ is within a geminate ion pair, an exciplex, or solvated. These situations can be differentiated from the time dependence of the band intensity (vide infra).

The 580 nm band is not due to $MNA^{\bullet+}$, which absorbs weakly around 700 nm and is hidden by $DCA^{\bullet-}$.[18] The dimer cation of naphthalene has been reported to absorb at this wavelength[19,20] and therefore this band is certainly due to $MNA_2^{\bullet+}$. Because of the weak extinction coefficients of $MNA^{\bullet+}$ and $MNA_2^{\bullet+}$ compared with those of ^{1}DCA* and $DCA^{\bullet-}$ (ϵ(700 nm) = 9000 M^{-1} cm^{-1}),[21] the detailed conversion kinetics from the 1:1 to the 1:2 complex cannot be determined. In order to study the kinetics of $MNA_2^{\bullet+}$ formation in more detail, the system CA/MNA in MeCN was investigated. ^{3}CA* is a strong enough acceptor to oxidize MNA and does not absorb in the region of interest.[20] Figure 2A shows the TG spectra measured at different time delays after excitation of CA at 355 nm in the presence of 0.25 M MNA in MeCN. In this case, the band located between 650 and 720 nm pertains to $MNA^{\bullet+}$ only.[18] The decrease of its intensity is accompanied by the formation of the 580 nm band, which can now be safely ascribed to $MNA_2^{\bullet+}$. The strong band which appears at shorter wavelength is due to ^{3}CA* (λ_{max} = 510 nm),[22] $CA^{\bullet-}$ absorbing at even shorter wavelength (λ_{max} = 450 nm).[18] As the diffracted intensity is proportional to the square of concentration changes,

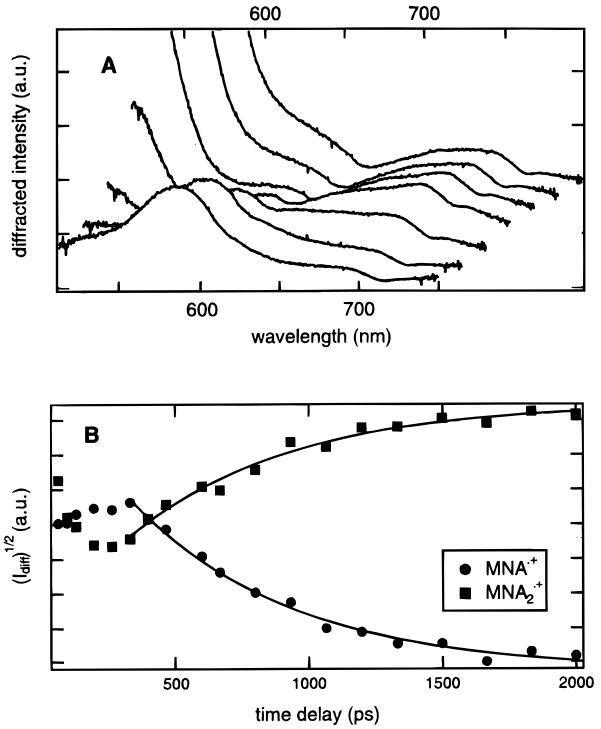

Figure 2. (A) Diffracted spectra measured at different time delays after excitation at 355 nm of a solution of CA and 0.25 M MNA in MeCN (from top to bottom: Δt = 60, 100, 200, 330, 600, 1200, and 1800 ps). The bottom and top wavelength axes refer to the bottom and top TG spectra, respectively. (B) Time dependence of the square of the diffracted intensities, $I_{diff}^{1/2}$, at 700 nm (MNA$^{\bullet+}$) and 580 nm (MNA$_2^{\bullet+}$) and best single-exponential fits (solid lines).

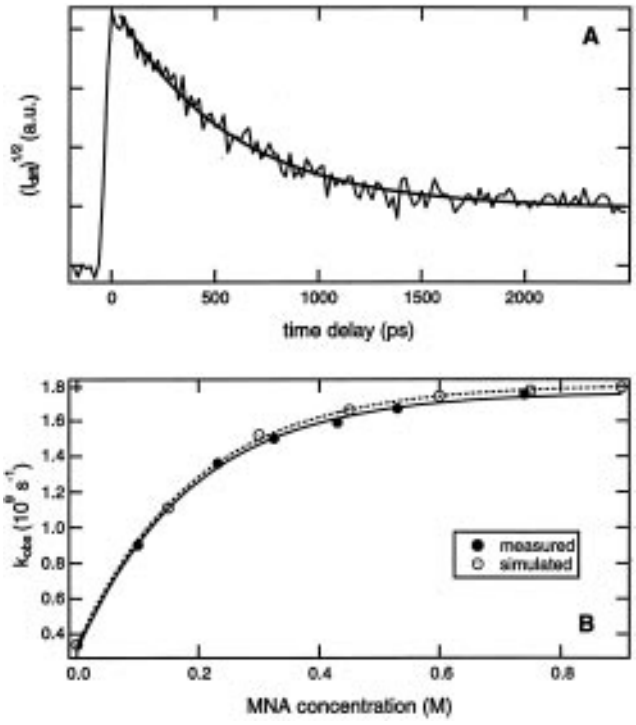

Figure 3. (A) Time profile of the square of the diffracted intensity, $I_{diff}^{1/2}$, at 681 nm measured with a solution of DCA and 0.53 M MNA in MeCN and best single-exponential fit. (B) MNA concentration dependence of the measured rate constant of GIP decay, k_{obs} (full circles) with the best-fitted exponential function (solid line) and of the rate constant obtained from simulation of eq 4 (empty circles) with the corresponding fitted exponential function (dashed line).

the kinetics of MNA$^{\bullet+}$ decay and MNA$_2^{\bullet+}$ formation can be obtained from the time dependence of the square root of the diffracted intensities at 700 and 580 nm, respectively, as shown in Figure 2B. The kinetics at short time delay is dominated by ET quenching, i.e., by the decay of ^{3}CA* and the formation of MNA$^{\bullet+}$. The fit of both kinetics at longer time delays results in the same rate constant, which gives a second-order rate constant for the reaction (CA$^{\bullet-}$·MNA$^{\bullet+}$) + MNA → (CA$^{\bullet-}$·MNA$_2^{\bullet+}$) of $k_{sq} = 6.8 \times 10^9$ M^{-1} s^{-1}. This rate constant is close to those reported for the self-quenching reactions of exciplexes composed of DCA and naphthalene or methylated naphthalene in MeCN, obtained from the concentration dependence of the exciplex fluorescence intensity.[5] This indicates that this process is not very sensitive to the nature of the electron acceptor. By comparing the TG band intensity of MNA$^{\bullet+}$ and MNA$_2^{\bullet+}$ with that of CA$^{\bullet-}$ (ϵ(450 nm) = 9700 M^{-1} cm^{-1}),[23] the extinction coefficients of MNA$^{\bullet+}$ and MNA$_2^{\bullet+}$ were determined to be equal to about 3000 and 3900 M^{-1} cm^{-1} at 694 and 580 nm, respectively.

Coming back to the DCA/MNA couple, Figure 3A shows the time dependence of the square root of the diffracted intensity at 681 nm with 0.53 M MNA. For the sake of clarity, the 1:1 and 1:2 complexes will be assumed to be geminate ion pairs and will be called GIP1 and GIP2, respectively. The exact nature of these species (CIP-like exciplex or LIP) will be discussed later. At 681 nm, the diffracted intensity reflects essentially the dynamics of DCA$^{\bullet-}$, within GIP1 or GIP2 or as a free ion (FI). This time profile can be very well fitted using a single exponential function decaying with a rate constant k_{obs} to a constant positive intensity, which is larger that the intensity prior to excitation. The monoexponential component is due to the decay of the geminate ion pairs by both charge recombination (CR) to the neutral ground state and separation to free ions. The remaining intensity pertains to the free ions, which decay

SCHEME 1

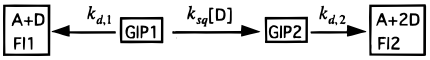

on the microsecond time scale by homogeneous recombination. These measurements were carried out at MNA concentrations ranging from 0.1 to 0.7 M. As donor concentration was increased, a substantial increase of k_{obs} was observed. This effect was accompanied by a decrease of the intensity related to free ions. This concentration dependence of k_{obs} is illustrated in Figure 3B. This behavior can be rationalized by considering that the decay rate constant of GIP1, $k_{d,1}$, is slower that the decay rate constant of GIP2, $k_{d,2}$ (see Scheme 1). Neglecting exciplex fluorescence of GIP1 which has a quantum yield of less than 1% and assuming that the back reaction from GIP2 to GIP1 is insignificant, as suggested by the measurements with CA and by the equilibrium constant observed between naphthalene cation and naphthalene dimer cation in benzonitrile,[24] the solutions of the differential equations for this coupled reactions are[25]

$$[\mathrm{GIP1}] = [\mathrm{GIP1}]_0 e^{-(k_{d,1}+k_{sq}[\mathrm{D}])t} \quad (1)$$

$$[\mathrm{GIP2}] = [\mathrm{GIP1}]_0 \gamma \{e^{-k_{d,2}t} - e^{-(k_{d,1}+k_{sq}[\mathrm{D}])t}\} \quad (2)$$

with

$$\gamma = \frac{k_{sq}[\mathrm{D}]}{k_{d,1} - k_{d,2} + k_{sq}[\mathrm{D}]} \quad (3)$$

The time dependence of the observable signal due to the GIP, with [GIP] = [GIP1] + [GIP2], is given by

$$[\mathrm{GIP}] = (1-\gamma)[\mathrm{GIP1}]_0 e^{-(k_{d,1}+k_{sq}[\mathrm{D}])t} + \gamma[\mathrm{GIP1}]_0 e^{-k_{d,2}t} \quad (4)$$

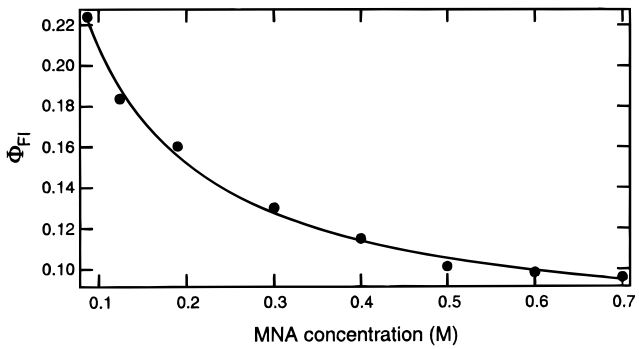

Figure 4. Concentration dependence of the free ion yield normalised to 100% DCA* quenching and best fit of eq 6 (solid line).

This equation predicts a two-exponential decay of the signal due to the geminate ion pairs except in the low and high concentration limits, where the decay is monoexponential with a rate constant equal to $k_{d,1}$ and $k_{d,2}$, respectively. Consequently, these two rate constants can in principle be recovered by extrapolating the concentration dependence of k_{obs} to both zero and infinite MNA concentrations. While a good estimate of $k_{d,2}$ can easily be obtained, the extrapolation to zero concentration is less straightforward. Equation 4 has been simulated using various values for $k_{d,n}$ and a value of 6.8×10^9 M^{-1} s^{-1} for k_{sq}. Apart from the very first stage of the decay, the simulated kinetics can be well fitted assuming a first-order decay with a rate constant increasing exponentially from $k_{d,1}$ to $k_{d,2}$ with increasing donor concentration.

If the measured MNA concentration dependence of k_{obs} is extrapolated using an exponential function, values for $k_{d,1}$ and $k_{d,2}$ of 3.4×10^8 and 1.8×10^9 s^{-1}, respectively, are obtained. Figure 3B shows the concentration dependence of the GIP decay simulated using eq 4 with these two $k_{d,n}$ values. The good agreement between the observed and simulated dependences supports strongly the use of Scheme 1.

Figure 4 shows the free ions yield normalised to 100% DCA* quenching, i.e., the separation efficiency, measured as a function of MNA concentration. As could be anticipated from the concentration dependence of k_{obs}, the free ion yield, Φ_{FI}, decreases substantially with increasing donor concentration. Free ions can be generated from both GIP1 and GIP2; therefore, Φ_{FI} is given by

$$\Phi_{FI} = \Phi_{FI,1} + \Phi_{FI,2} = \Phi_{GIP1}\Phi_{sep,1} + \Phi_{GIP2}\Phi_{sep,2} \quad (5)$$

where Φ_{sep1} and Φ_{sep2} are the separation efficiencies of GIP1 and GIP2. Assuming 100% quenching of DCA*, i.e., $\Phi_{GIP} = \Phi_{GIP1} + \Phi_{GIP2} = 1$:

$$\Phi_{FI} = \Phi_{sep,1} - (\Phi_{sep,1} - \Phi_{sep,2})\Phi_{GIP2} \quad (6)$$

with

$$\Phi_{GIP2} = \frac{k_{sq}[D]}{k_{sq}[D] + k_{d,1}} \quad (7)$$

The fit of eq 6 to the experimental free ion yields using the above-determined values of $k_{d,1}$ and k_{sq} results in efficiencies of 0.47 and 0.06 for the separation of GIP1 and GIP2, respectively.

Discussion

The physical meaning of the $k_{d,n}$ rate constants depends on the nature of GIP1 and GIP2. The ion pair dynamics is often discussed in terms of CIP and of LIP.[26−32] The observation of exciplex fluorescence and self-quenching by Gould and Farid with similar donors indicates that the primary product of DCA fluorescence quenching by MNA is a 1:1 CIP-like exciplex (CIP1).[4] Similarly, the product of self-quenching by a second MNA molecule is a 1:2 CIP (CIP2). As shown by Scheme 2, these CIPs can either recombine to the neutral ground state or separate to LIPs. Moreover, LIP1 and FI1 can also be converted to LIP2 and FI2 upon reaction with a second donor molecule. The second-order rate constants for these processes (k'_{sq} and k''_{sq} in Scheme 2) can be expected to lie between k_{sq} and the diffusion constant. In order to extract the CR and ion pair separation rate constants from the $k_{d,n}$ values, two different models will be considered.

SCHEME 2

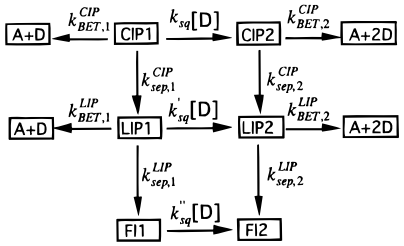

Model 1. CR essentially takes place within the CIPs. In this case, the LIPs do not play a significant role and the CIPs decay by back ET to the neutral ground state ($k^{CIP}_{BET,n}$) and by separation to the free ions ($k^{CIP}_{sep,n}$) through the LIP. These rate constants can be estimated from the $k_{d,n}$ values and from the separation efficiencies, $\Phi_{sep,n}$, at the low and high donor concentration limits. The separation efficiency is defined as

$$\Phi_{sep,n} = \frac{k^{CIP}_{sep,n}}{k_{d,n}} = \frac{k^{CIP}_{sep,n}}{k^{CIP}_{sep,n} + k^{CIP}_{BET,n}} \quad (8)$$

From the $\Phi_{sep,n}$ values and eq 8, $k^{CIP}_{sep,1}$ and $k^{CIP}_{sep,2}$ are equal to 1.6×10^8 and 1.1×10^8 s^{-1}, respectively, and the rate constant of back ET within the CIPs, $k^{CIP}_{BET,1}$ and $k^{CIP}_{BET,2}$ amounts to 1.8×10^8 and 1.7×10^9 s^{-1}, respectively.

Model 2. According to Gould and Farid,[5] the reorganization energy for CR in a 1:1 CIP is very small and therefore back ET is far in the inverted region. Consequently, back ET within CIP1 should be very slow and inefficient ($k^{CIP}_{BET,1} < 10^7$ s^{-1}) and CR takes only place through LIP1. On the other hand, the solvent reorganization energy of a 1:2 CIP is close to that of a 1:1 LIP and therefore the CR in the 1:2 complex essentially takes place within CIP2. The experimental data described here can fit to this scheme if the decay rate constant of LIP1 is equal or larger than that of CIP1; i.e., LIP1 is consumed as soon as it is formed. In this case, the total population CIP1 + LIP1 (i.e., GIP1) decays monoexponentially with a rate constant $k_{d,1}$ corresponding to $k^{CIP}_{sep,1}$, which is then equal to 3.4×10^8 s^{-1}. The separation efficiency, $\Phi_{sep,1}$, is now given by

$$\Phi_{sep,1} = \frac{k^{LIP}_{sep,1}}{k^{LIP}_{sep,1} + k^{LIP}_{BET,1}} \quad (9)$$

In this case, only lower limit values can be obtained, i.e., $k^{LIP}_{BET,1} \geq 3.4 \times 10^8$ and $k^{LIP}_{sep,1} \geq 3.0 \times 10^8$ s^{-1}. At the high concentration limit, only CIP2 is generated. As the population decay is monoexponential within the experimental error, CR must take place within CIP2 only. Therefore, the values of $k^{CIP}_{BET,2}$ and $k^{CIP}_{sep,2}$ are the same as those obtained in model 1.

TABLE 1

	model 1	model 2
$k^{CIP}_{BET,1}$ (s^{-1})	1.8×10^8	$<10^7$
$k^{CIP}_{BET,2}$ (s^{-1})	1.7×10^9	1.7×10^9
$k^{CIP}_{sep,1}$ (s^{-1})	1.6×10^8	3.4×10^8
$k^{CIP}_{sep,2}$ (s^{-1})	1.1×10^8	1.1×10^8
$k^{LIP}_{BET,1}$ (s^{-1})	$\ll 1.8 \times 10^8$	$\geq 3.4 \times 10^8$
$k^{LIP}_{BET,2}$ (s^{-1})	$\ll 1.1 \times 10^8$	$\ll 1.1 \times 10^8$
$k^{LIP}_{sep,1}$ (s^{-1})	$\geq 1.6 \times 10^8$	$\geq 3.0 \times 10^8$
$k^{LIP}_{sep,2}$ (s^{-1})	$\geq 1.1 \times 10^8$	$\geq 1.1 \times 10^8$

The values of the various rate constants involved in these two models are listed in Table 1. On the basis of these data, none of these models can definitely be rejected. Model 2 is based on the assumption that CR in CIP is very slow for the reasons given above. However, there have been many observations of rate constants for back ET within CIPs larger than 10^{10} s^{-1}.[33-37] Comparatively, a value for $k^{CIP}_{BET,1}$ of 1.8×10^8 s^{-1} is very small and can well correspond to a back ET far in the inverted region. The dimer cation $MNA_2^{\bullet+}$ has been measured to be 0.11 eV more stable than the monomer cation MNA^{+}.[38] Consequently, back ET within CIP2 is less exergonic than within CIP1 and $k^{CIP}_{BET,2}$ is larger than $k^{CIP}_{BET,1}$. Moreover, as CIP1 and CIP2 have rather different structures, the reorganization energies, and especially that associated to solvent coordinates and low-frequency modes, λ_s, can also be expected to be different. If, as suggested by Gould and Farid,[5] λ_s is smaller for CIP1 than for CIP2, the inverted region for $k^{CIP}_{BET,1}$ will be shifted toward lower exergonicities relative to that for $k^{CIP}_{BET,2}$. This should further lead to slower back ET for CIP1 compared with CIP2. Within model 2, the differences in λ_s have to be much larger to account for the difference between $k^{CIP}_{BET,1}$ and $k^{CIP}_{BET,2}$.

The relative magnitude of the rate constants of separation for CIP1 and CIP2 seems physically more realistic with model 1. Indeed, $k^{CIP}_{sep,n}$ is essentially a diffusional process with an activation energy related to viscosity and to the electrostatic interaction between the ions. If the sizes of the ions are considered, the diffusion constant of $MNA^{\bullet+}$ must be approximately twice as large as that of $MNA_2^{\bullet+}$. If $k^{CIP}_{sep,n}$ is taken as the sum of the diffusion constants of the ions, $k^{CIP}_{sep,1}$ must be 50% larger than $k^{CIP}_{sep,2}$, as obtained from model 1. If the electrostatic interaction is taken into account, the difference could even be smaller. Indeed, a slightly weaker interaction in CIP2 due to the larger delocalization of the positive charge can be expected. According these considerations, the relative magnitude of $k^{CIP}_{sep,n}$ obtained from model 2 is more difficult to account for.

Conclusions

Using TG spectroscopy, we have been able to monitor the dynamics of the ion pairs involved in the ET reaction between DCA and MNA. The dependence of the ion population dynamics on quencher concentration can be well accounted for with a scheme involving the coupled reactions, with rate constants $k_{d,n}$, of two ion pairs or two groups of ion pairs (see Scheme 1). However, in order to extract the rate constants of CR and separation from these $k_{d,n}$ values, a more detailed scheme has to be used. In our opinion, a model where forward ET and back ET essentially take place at contact distance results in physically more reasonable rate constants for CR and ion pair separation. However, the involvement of a LIP in the CR within the 1:1 complex cannot be ruled out.

Acknowledgment. This work was supported by the Fonds national suisse de la recherche scientifique through project no. 20-41855.94 and by the Programme d'encouragement à la relève universitaire de la Confédération. Financial support from the Fonds de la recherche and the Conseil de l'Université de Fribourg is also acknowledged.

References and Notes

(1) Fox, M. A.; Chanon, M. *Photoinduced Electron Transfer*; Elsevier: Amsterdam, 1988.
(2) Gould, I. R.; Ege, D.; Mattes, S. L.; Farid, S. *J. Am. Chem. Soc.* **1987**, *109*, 3794.
(3) Vauthey, E.; Suppan, P.; Haselbach, E. *Helv. Chim. Acta* **1988**, *71*, 93.
(4) Gould, I. R.; Young, R. H.; Mueller, L. J.; Farid, S. *J. Am. Chem. Soc.* **1994**, *116*, 8176.
(5) Gould, I. R.; Farid, S. *J. Am. Chem. Soc.* **1993**, *115*, 4814.
(6) Schneider, S.; Geiselhart, P.; Seel, G.; Lewis, F. D.; Dykstra, R. E.; Nepras, M. J. *J. Phys. Chem.* **1989**, *93*, 3112.
(7) Saltiel, J.; Townsend, D. E.; Watson, B. D.; Shannon, P.; Finson, S. L. *J. Am. Chem. Soc.* **1977**, *99*, 884.
(8) Beens, H.; Weller, A. *Chem. Phys. Lett.* **1968**, *2*, 3.
(9) Högemann, C.; Pauchard, M.; Vauthey, E. *Rev. Sci. Instrum.* **1996**, *67*, 3449.
(10) Vauthey, E. *Chem. Phys. Lett.* **1993**, *216*, 530.
(11) Vauthey, E.; Henseler, A. *J. Phys. Chem.* **1995**, *99*, 8652.
(12) Vauthey, E.; Pilloud, D.; Haselbach, E.; Suppan, P.; Jacques, P. *Chem. Phys. Lett.* **1993**, *215*, 264.
(13) von Raumer, M.; Suppan, P.; Jacques, P. *J. Photochem. Photobiol. A*, in press.
(14) Henseler, A.; Vauthey, E. *J. Photochem. Photobiol. A* **1995**, *91*, 7.
(15) Perrin, D. D.; Armarego, W. L. F.; Perrin, D. R. *Purification of Laboratory Chemicals*; Pergamon Press: Oxford, U.K., 1980.
(16) Haselbach, E.; Jacques, P.; Pilloud, D.; Suppan, P.; Vauthey, E. *J. Phys. Chem.* **1991**, *95*, 7115.
(17) Haselbach, E.; Vauthey, E.; Suppan, P. *Tetrahedron* **1988**, *44*, 7335.
(18) Shida, T. *Electronic Absorption Spectra of Radical Ions*; Elsevier: Amsterdam, 1988.
(19) Rodgers, M. A. J. *J. Chem. Soc. Faraday Trans. 1* **1972**, 1278.
(20) Gschwind, R.; Haselbach, E. *Helv. Chim. Acta* **1979**, *62*, 941.
(21) Gould, I. R.; Ege, D.; Moser, J. E.; Farid, S. *J. Am. Chem. Soc.* **1990**, *112*, 4290.
(22) Carmichael, I.; Hug, G. L. *J. Phys. Chem. Ref. Data* **1986**, *15*, 1.
(23) André, J. J.; Weill, G. *Mol. Phys.* **1968**, *15*, 97.
(24) Kira, A.; Arai, S.; Imamura, M. *J. Phys. Chem.* **1972**, *76*, 1119.
(25) Demas, J. N. *Excited State Lifetime Measurements*; Academic Press: New York, 1983.
(26) Winstein, S.; Robinson, G. C. *J. Am. Chem. Soc.* **1958**, *80*, 169.
(27) Szwarck, M. *Acc. Chem. Res.* **1969**, *2*, 87.
(28) Weller, A. *Pure Appl. Chem.* **1982**, *54*, 1885.
(29) Simon, J. D.; Peters, K. S. *J. Am. Chem. Soc.* **1982**, *104*, 6142.
(30) Masnovi, J. M.; Kochi, J. K. *J. Am. Chem. Soc.* **1985**, *107*, 7880.
(31) Asahi, T.; Mataga, N. *J. Phys. Chem.* **1989**, *93*, 6575.
(32) Gould, I. R.; Young, R. H.; Moody, R. E.; Farid, S. *J. Phys. Chem.* **1991**, *95*, 2068.
(33) Asahi, T.; Mataga, N.; Takahashi, Y.; Miyashi, T. *Chem. Phys. Lett.* **1990**, *171*, 309.
(34) Hubig, S. M. *J. Phys. Chem.* **1992**, *96*, 2903.
(35) Peters, K. S.; Lee, J. *J. Am. Chem. Soc.* **1993**, *115*, 3643.
(36) Wynne, K.; Galli, C.; Hochstrasser, R. M. *J. Chem. Phys.* **1994**, *100*, 4797.
(37) Hubig, S. M.; Bockman, T. M.; Kochi, J. K. *J. Am. Chem. Soc.* **1996**, *118*, 3842.
(38) Terahara, A.; Ohya-Nishiguchi, H.; Hirota, N.; Oku, A. *J. Phys. Chem.* **1986**, *90*, 1564.